Altered basal forebrain regulation of intrinsic brain networks in depressive and anxiety disorders

*Alec J. Jamieson [1], Trevor Steward [1,2], Christopher G Davey [1], Sevil Ince [1,2], James A Agathos [1], Bradford A Moffat [3], Rebecca K Glarin [3], Kim L Felmingham [2], Ben J Harrison[1]

[1] Department of Psychiatry, The University of Melbourne, Parkville, Australia

[2] Melbourne School of Psychological Sciences, The University of Melbourne, Parkville, Australia

[3] The Melbourne Brain Centre Imaging Unit, Department of Radiology, The University of Melbourne, Parkville, Australia

***Corresponding author:** Dr. Alec Jamieson. Department of Psychiatry, The University of Melbourne. Level 3, 161 Barry St. Carlton, VIC 3053. Phone: (+61) 449 501 556 | Email: alec.jamieson@unimelb.edu.au

Keywords: Basal forebrain; Effective connectivity; Depressive disorders; Anxiety disorders; Resting-state

Word count: 4430

Abstract

Altered connectivity both within and between the default mode and salience networks have been observed across depressive and anxiety disorders. Recent work has highlighted the importance of subcortical regions, including subdivisions of the basal forebrain, in coordinating activity of these networking. However, the influence of specific basal forebrain subregions on intrinsic networks across these disorders remains unknown. Using ultra-high field (7-Tesla) functional magnetic resonance imaging, we examined the resting-state effective connectivity of three basal forebrain subregions in a transdiagnostic group of 70 individuals with depressive and anxiety disorders compared to 78 healthy controls. We explored connectivity between these subregions and regions of the salience network (anterior insula and dorsal anterior cingulate) and default mode network (ventromedial prefrontal cortex, posterior cingulate cortex, and inferior parietal lobule). Clinical participants showed increased inhibitory connectivity from the nucleus basalis of Meynert to regions of the default mode network and dorsal anterior cingulate. Increased inhibitory connectivity was also observed from the ventral pallidum to regions of the posterior default mode network. These changes in the basal forebrain's regulation of large-scale cortical networks across depressive and anxiety disorders may suggest novel mechanistic avenues for pharmacological treatments, including cholinergic system targeting.

Widespread alterations to intrinsic brain network activity have been noted across depressive and anxiety disorders (Dutta et al. 2014; Bertocci et al. 2023; Zhang et al. 2023). Specifically, these mental health conditions have been predominately associated with connectivity changes in the default mode (DMN) and salience networks (Mulders et al. 2015). Abnormal DMN connectivity in major depressive disorder (MDD) has been associated with higher levels of rumination and an increased duration of depressive episodes (Mohan et al. 2016). Moreover, altered resting-state connectivity, both within the DMN and between the DMN and salience network, has been observed across both social and generalized anxiety disorders (Rabany et al. 2017) and associated with anxiety symptom severity (Li et al. 2023). Abnormal functioning of these networks has been hypothesized to relate to common symptoms across both conditions. For example, DMN alterations are suggested to contribute to abnormal self-referential processing and rumination, whereas dysfunction in the salience network is related to abnormal processing of negative stimuli (Xu et al. 2021; Jamieson et al. 2022; Jamieson et al. 2023). Dysfunction within and between these networks may therefore be a transdiagnostic feature across depressive and anxiety disorders.

Although the DMN and salience networks are primarily identified as cortical in nature, there is emerging evidence that their function is heavily influenced by subcortical modulatory structures, including the basal forebrain (Nair et al. 2018; Alves et al. 2019; Aguilar and McNally 2022). The basal forebrain's influence over the DMN has been hypothesized to reflect a mechanism for switching between internally and externally directed attention states (Nair *et al.* 2018; Harrison et al. 2022). Activation of cholinergic neurons in the basal forebrain of rodents has also been shown to decrease DMN functional connectivity, highlighting a potential role of the basal forebrain in regulating the activity of this network (Peeters et al. 2020). Notably, the cholinergic component of the basal forebrain demonstrates distinct subdivisions with heterogeneity demonstrated in both their histochemistry and

function (Mesulam et al. 1983). These subregions include the medial septal nucleus (cholinergic group 1; Ch1), vertical nucleus of the diagonal band (Ch2), horizontal nucleus of the diagonal band (Ch3), and nucleus basalis of Meynert (Ch4) (Mesulam *et al.* 1983). Notably, Ch4 demonstrates the highest concentration of cholinergic cells, comprising approximately 90% of its neurons, and represents the major source of cholinergic innervation for the cortical mantle (Mesulam *et al.* 1983). These basal forebrain subdivisions are largely replicated in resting-state fMRI functional connectivity studies, with Fritz and colleagues illustrating two functional subcomponents congruent with Ch1-3 and Ch4 (Fritz et al. 2019). Importantly these subregions demonstrate differential connectivity patterns with intrinsic cerebral networks, with Ch1-3 exhibiting a strong functional connectivity with the anterior DMN, whereas Ch4 activity is correlated with the functioning of the salience and central executive networks (Li et al. 2014; Fritz *et al*. 2019; Yuan et al. 2019). In contrast, the ventral pallidum (VP), a basal forebrain subregion which is predominately GABAergic (Root et al. 2015), has also demonstrated evidence for controlling transitions between internally and externally guided behavior by regulating DMN activity (Klaassen et al. 2021; Aguilar and McNally 2022; Zhao et al. 2024). This indicates that different subregions of the basal forebrain likely have distinct and overlapping roles in coordinating the activity of different intrinsic brain networks, however, investigations into whether specific subregions are altered in depressive and anxiety disorders remains limited.

The basal forebrain is implicated in functions that are known to be altered across depression and anxiety, including the modulation of circadian rhythms, appetite, motivation, and cognitive flexibility (Cabrera et al. 2006; Herman et al. 2016; Yamakawa et al. 2016). There is also consistent evidence that reductions in acetylcholinesterase activity and increasing acetylcholine levels can induce depression and anxiety symptoms in humans and rodents (Mineur et al. 2013; Dulawa and Janowsky 2019). Rodent work suggests that both

lesions in cholinergic neurons and stress-induced hyperactivity of VP GABAergic neurons can produce depression-like behaviors (Knowland et al. 2017; Chen et al. 2021). Importantly, depression-like behaviors induced by cholinergic lesions appear reversable with both ketamine and fluoxetine treatment (Chen *et al.* 2021). Together this indicates that core basal forebrain disturbances may be present across anxiety and depressive disorders and drive changes in cortical brain regions. However, research on the functioning of the basal forebrain and its subregions remains limited in humans due to the technical limitations of conventional (3-Tesla) fMRI approaches (Keuken et al. 2018).

To address this gap, we examined the role of basal forebrain subregions, specifically Ch1-3, Ch4, and VP, in coordinating the activity of regions of the DMN and salience network using ultra high field (7-Tesla) fMRI to enhance spatial and temporal resolution capability. We used spectral dynamic causal modeling (DCM) [31] to examine alterations in the basal forebrain's regulatory influence over intrinsic networks in individuals with depressive and anxiety disorders. Given the growing evidence for the role of Ch1-3, 4, and VP in the coordination (Klaassen *et al.* 2021; Aguilar and McNally 2022; Zhao *et al.* 2024). We hypothesized that these disorders would be characterized by greater influence from basal forebrain regions to the DMN, particularly from Ch4 and the VP, consistent with . We additionally hypothesized that altered effective connectivity (i.e., directional influences among brain regions) would be associated with depression and anxiety symptom severity.

Methods

A transdiagnostic sample of 79 clinical participants were recruited to the study from The University of Melbourne Psychology Clinic and via the Research Experience Program at the Melbourne School of Psychological Sciences. All clinical participants underwent the Diagnostic Interview for Anxiety, Mood, and OCD and Related Neuropsychiatric Disorders

(DIAMOND) (Tolin et al. 2016), a semi-structured clinical interview based on DSM-5 diagnostic criteria, to confirm the presence of a mood and/or anxiety disorder. Participants who met criteria for psychosis, bipolar disorder, somatic symptom disorder, paraphilic disorder, dissociative disorder, conduct disorder, neurodevelopmental disorders, or substance use disorder were excluded. Reported anxiety disorders included generalized anxiety disorder, social anxiety disorder, panic disorder, or specific phobias, while depressive disorders included major depressive disorder, persistent depressive disorder, premenstrual dysphoric disorder, or major depressive episode. Clinical participants were compared to 92 matched control participants recruited via publicly accessible online advertisements. These participants had no current or past diagnosis of a mental health disorder as assessed through the Mini-International Neuropsychiatric Interview-7 (Sheehan et al. 1998). All participants were between 18 to 40 years of age, fluent English speakers, had no MRI contraindications including pregnancy, and had normal or corrected-to-normal visual acuity. All participants provided written informed consent prior to the study, following a complete description of the study protocol. This study and its protocol were approved by the Melbourne Health Human Research and Ethics Committee. All participants attended a single session at the Melbourne Brain Imaging Unit (The University of Melbourne, Parkville). The Depression, Anxiety and Stress Scale short-form (DASS-21) was administered prior to the session to provide an overall measure of negative mood states, as well as sub-scales scores of depression, anxiety, and stress-tension (Lovibond 1995). Of the original sample, three participants were excluded due to data quality issues (three controls), five participants were excluded due to excessive head movement during scanning (four controls and one clinical participant), and 15 due to insufficient activity mapping across all regions necessary for DCM (10 controls and five clinical participants; for further details see Times Series Extraction below). This resulted in 70 clinical participants and 78 healthy controls being included in the primary analysis.

Image Acquisition

MRI acquisition was performed on a Siemens 7T Plus research scanner (Siemens Healthcare, Erlangen, Germany) equipped with a 32Rx/1Tx channel head coil (Nova Medical Inc., Wilmington MA, USA). Functional (T2*-weighted) images were obtained using a multi-band and grappa accelerated gradient-echo planar imaging (GE-EPI) sequence (Moeller et al. 2010) in the steady state (multi-band factor, 6; parallel acceleration factor, 2; repetition time, 800 ms; echo time, 22.2 ms; flip angle, 45°) in a 20.8 cm field-of-view, with a 130×130-pixel matrix, a slice thickness of 1.6mm (no gap) and in-plane voxel size=1.6×1.6 mm. Eighty-four interleaved slices were acquired parallel to the anterior-posterior commissure line, covering the whole brain. The resting-state sequence duration was 5 minutes and 20 seconds, corresponding to 400 whole-brain echo-planar imaging volumes. Participants were instructed to keep their eyes closed but not to fall asleep for the duration of the scan.

A high resolution structural T1-weighted image was obtained from each participant using magnetization-prepared 2 rapid gradient echo sequence (MP2RAGE (Marques et al. 2010)) for co-registration with the functional images (parallel reduction factor, 4; repetition time, 5 seconds; echo time, 2.04 ms; flip angle, 13°) in a 24 cm field of view, with a 330×330–pixel matrix, in-plane voxel size = 0.75×0.75 mm, slice thickness = 0.75 mm with 224 sagittal slices aligned parallel to the midline. To minimize head movement during scanning, foam pads were inserted to the either side of participants' heads. Respiration and cardiac pulse were also recorded during the session at 200 hertz (Hz) and 50 Hz, respectively, using a respiratory belt and pulse-oximeter (Siemens, Germany) to be used for physiological noise correction.

Preprocessing

Imaging data were preprocessed using Statistical Parametric Mapping (SPM) 12 (v7771, Welcome Trust Centre for Neuroimaging, London, UK) within a MATLAB 2023b environment (The MathWorks Inc., Natick, MA) on Spartan High Performance Computer hosted at The University of Melbourne (Lafayette et al. 2016). Motion artifacts were corrected by realigning each participant's timeseries to the mean image, and all images were resampled using 4th Degree B-Spline interpolation. Participants were excluded if movement exceeded a mean total displacement of 1.6mm (~1 native voxel) as assessed through the Motion Fingerprint toolbox (Wilke 2012).

Each participant's anatomical images (denoised MP2RAGE (O'Brien et al. 2014)) were co-registered to their respective mean functional image, segmented, and normalized to the International Consortium of Brain Mapping template using the unified segmentation and the Diffeomorphic Anatomical Registration Through Exponentiated Lie Algebra approach (Ashburner 2007). Smoothing was applied with a 3.2-mm^3 full-width-at-half-maximum Gaussian kernel to preserve spatial specificity. Physiological noise was modeled using PhysIO toolbox (Kasper et al. 2017). Cardiac and respiratory recordings were imported to the toolbox, in which physiological noise models were applied to these recordings (i.e., the retrospective image-based correction for a third order cardiac, fourth order respiratory, and first order interaction Fourier expansion of cardiac and respiratory phase (Glover et al. 2000); respiratory volume per time (Birn et al. 2008); heart rate variability response (Chang et al. 2009)). Normalized white matter and cerebrospinal fluid tissue segmentations from each participant's structural image were used to construct noise regions of interest from which mean timeseries and principal components were extracted as nuisance regressors using CompCor (Behzadi et al. 2007). These regressors were added to six movement regressors estimated through realignment and taken to the first-level general linear model to remove variances of no-interest.

Spectral Dynamic Causal Modeling

DCM is a technique used to infer directional influences among brain regions, or effective connectivity, based on functional neuroimaging data (Friston et al. 2003; Friston and Penny 2011). While traditional deterministic and stochastic DCM operates by analyzing the timeseries data directly, spectral DCM estimates effective connectivity using the cross-spectral density (for further details see Supplementary Methods). This is a second-order summary statistic of the timeseries data and thus allows the estimation of effective connectivity parameters for resting-state data with a greatly increased computational efficiency (Novelli et al. 2024). Effective connectivity between regions is measured in Hz, with positive values being indicative of putative excitation between regions while negative values represent putative inhibition. Self or within-region connections are represented by unitless log scaling parameters that modify the default inhibitory connectivity of -0.5Hz. As such, positive values for these parameters are indicative of greater inhibition whereas negative values represent reduced inhibition.

Timeseries Extraction and Model Specification

The Montreal Neurological Institute coordinates for core regions of the DMN and salience network were identified using previously reported peak coordinates from meta-analyses and large-scale functional connectivity studies. The precise coordinates were as follows: vmPFC [3, 39, -2] (Fair et al. 2009), PCC [2 -43 24] (Fair *et al.* 2009), IPL [44 -65 32; -40 -66 32] (Yarkoni et al. 2011), anterior insula [36, 16, 4; -35, 14, 5] (Dosenbach et al. 2007), dorsal anterior cingulate (dACC) [4, 30, 30] (Sridharan et al. 2008). The timeseries from these VOIs were extracted using the principal eigenvariate of all voxels in a sphere within a radius of 6 mm of the centroids for midline regions (vmPFC, PCC, dACC) and 4 mm for lateralized

regions (IPL and anterior insula; Supplementary Figure S1). To extract the basal forebrain subregions, we used basal forebrain masks based on the stereotaxic probabilistic maps of the magnocellular basal forebrain space by Zaborszky and colleagues (Zaborszky et al. 2008) for Ch1-3 and 4, and the subcortical mask from Pauli and colleagues (Pauli et al. 2018) for the VP (Figure 1). Seed-to-whole brain functional connectivity analyses were conducted to ensure that these masks accurately captured the intended regions and their associated functional connectivity patterns (Supplementary Methods and Results).

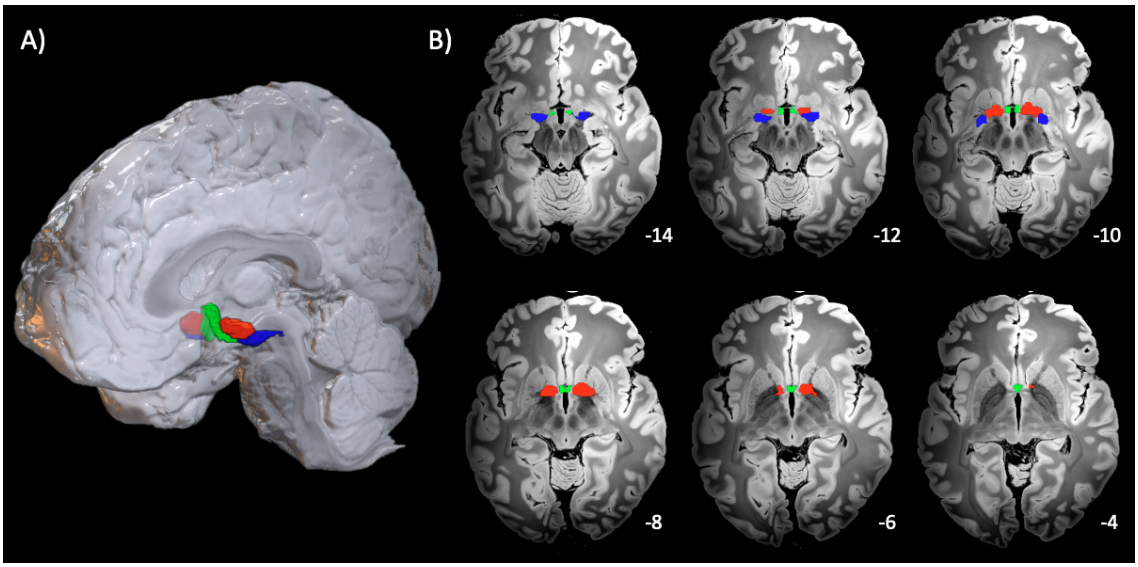

Figure 1. Basal forebrain masks used in the effective connectivity analysis. A) Render and B) axial slices of the Ch1-3 (green), Ch4 (blue), and VP (red) masks on the "Synthesized_FLASH25" (500 µm, MNI space) ex vivo template (Edlow et al. 2019).

Our model space was specified using DCM 12.5. To address our hypotheses concerning the distinct effects of basal forebrain subregions, we modeled bidirectional connectivity to and from these subregions to all cortical regions highlighted above. Using the *spm_dcm_fmri_check* function, we assessed the explained variance of the model. This revealed an average explained variance of 86.9% across all subjects, indicating that the

specified model was capturing a large degree of the observed changes in BOLD signal over time.

Parametric Empirical Bayes

To examine the impact of group differences on individual parameters, we employed Parametric Empirical Bayes (PEB) (Friston et al. 2016). Unlike comparisons using classical frequentist tests which only use estimated mean values, PEB allows for the inclusion of estimated variance (in addition to the estimated means) of each parameter when investigating between-group effects. The posterior probability (PP) was calculated using the free energy (with vs. without) option. This approach compares the evidence for all models in which a particular parameter is switched on with the evidence for models in which it is switched off. A PP threshold of greater than 0.99 was used to identify those parameters which had a *very strong* amount of evidence (Zeidman et al. 2019). We constructed a second level PEB model including four regressors. The first regressor modeled the average connectivity observed across healthy control participants, with subsequent regressors either increasing or decreasing this baseline connectivity. The subsequent regressors included the difference between clinical participants and healthy controls, as well as age and gender as covariates. Having estimated a group level PEB model, we then searched over nested PEB models using Bayesian model reduction pruning parameters that did not contribute to overall model evidence (Friston and Penny 2011; Rosa et al. 2012). Bayesian model averaging was performed on these models after the final iteration to determine the strength of connections in the last Occam's window of 256 models.

Leave-one-out Cross-validation

To assess the predictive validity of parameters which demonstrated between-group differences, we used leave-one-out cross-validation (LOOCV) across all participants. In the PEB framework, LOOCV aims to determine whether the size of between-group effects on parameters is sufficiently large to predict a variable of interest (Zeidman *et al.* 2019). In this case, this was employed to determine whether identified parameters were related to symptom severity. A group-level PEB model was estimated for all participants while excluding one participant, then this PEB model was used to predict the left-out subject's DASS scores. These predicted scores were then correlated with the observed symptom severity. A significant correlation between the expected and observed values demonstrates that the effect size was sufficiently large to predict the left-out subjects' symptom severity above chance (see (Zeidman *et al.* 2019) for further details).

Results

Demographic and Clinical Differences

As expected, clinical participants' scores were significantly greater than healthy controls on the total DASS scale and across all three subscales (Table 2). The proportion of female clinical participants was significantly higher than in the healthy control group ($X^2 = 12.26$, $p = .003$). However, there were no significant differences in DASS total scores between male and females within the healthy control ($t(75) = .84$, $p = .201$) or clinical groups ($t(28.86) = .05$, $p = .479$). No other demographic differences were observed between the two groups (Table 1).

Table 1.

Comparison of Characteristics Between Healthy Controls and Clinical Participants

	Healthy Controls (*N* = 78)		Clinical Participants (*N* = 70)			
Characteristics	Mean or N	*SD* or Percentage	Mean or N	*SD* or Percentage	Effect size (φ, Δ, or *d*)	*p*
Age (years)	22.78	4.1	22.29	5.3	.10	.264
Female	43	55.8	51	72.9	.28	.003
Antidepressant Use	-	-	14	19.7	-	-
Current Depressive Disorder	-	-	34	48.6	-	-
Past Depressive Disorder	-	-	19	27.1	-	-
Current Anxiety Disorder	-	-	32	45.7	-	-
Current PTSD	-	-	10	14.3	-	-
DASS Total	7.62	6.0	27.16	11.2	-1.74	<.001
DASS Depression	2.40	2.2	10.14	5.5	-1.78	<.001
DASS Anxiety	1.78	1.9	7.06	4.2	-1.26	<.001
DASS Stress	3.52	3.3	9.96	4.1	-2.10	<.001

Abbreviations: Depression Anxiety Stress Scale (DASS); Post-traumatic Stress Disorder (PTSD)

Effective Connectivity Differences in Clinical Participants and Healthy Controls

Overall, healthy controls demonstrated an excitatory influence from Ch1-3 over the vmPFC (0.20 Hz), PCC (0.12 Hz), left IPL (0.13 Hz) and VP (0.09 Hz) and an inhibitory influence

over the anterior insula (R: -0.40 Hz; L: -0.36 Hz) and dACC (-0.14 Hz). Ch4 illustrated an excitatory influence over the anterior insula (R:0.28 Hz; L:0.26 Hz) and VP (0.17 Hz) and an inhibitory influence over the vmPFC (-0.26 Hz), PCC (-0.54 Hz), and IPL (R: -0.55 Hz; L: -0.59 Hz). Finally, VP showed an excitatory influence over Ch1-3 (0.07 Hz), Ch4 (0.26 Hz), and the left anterior insula (0.11 Hz) and an inhibitory influence over the vmPFC (-0.20 Hz), PCC (-0.27 Hz), IPL (R: -0.40 Hz; L: -0.47 Hz).

Compared with healthy controls, clinical participants demonstrated strong evidence for greater inhibitory connectivity from Ch4 to the vmPFC (-0.30 Hz), dACC (-0.20 Hz), PCC (-0.24 Hz), and IPL (R: -0.27; L: -0.29; Figure 2A). Clinical participants also demonstrated greater excitatory connectivity from Ch4 to bilateral anterior insula (R: 0.13; Hz; L: 0.12 Hz) and from the left anterior insula to Ch4 (0.07 Hz), as well as reduced excitatory connectivity from Ch4 to VP (-0.12 Hz) and to Ch1-3 (-0.10 Hz).

Clinical participants were observed to have greater excitatory connectivity from the VP to the right anterior insula (0.21 Hz), whereas greater inhibitory connectivity was observed from the VP to the PCC (-0.14 Hz), and bilateral IPL (R: -0.27 Hz; L: -0.24 Hz). Reduced excitatory connectivity from the vmPFC (-0.06 Hz) and greater connectivity from the left anterior insula (-0.10 Hz) to the VP were also observed (Figure 2B).

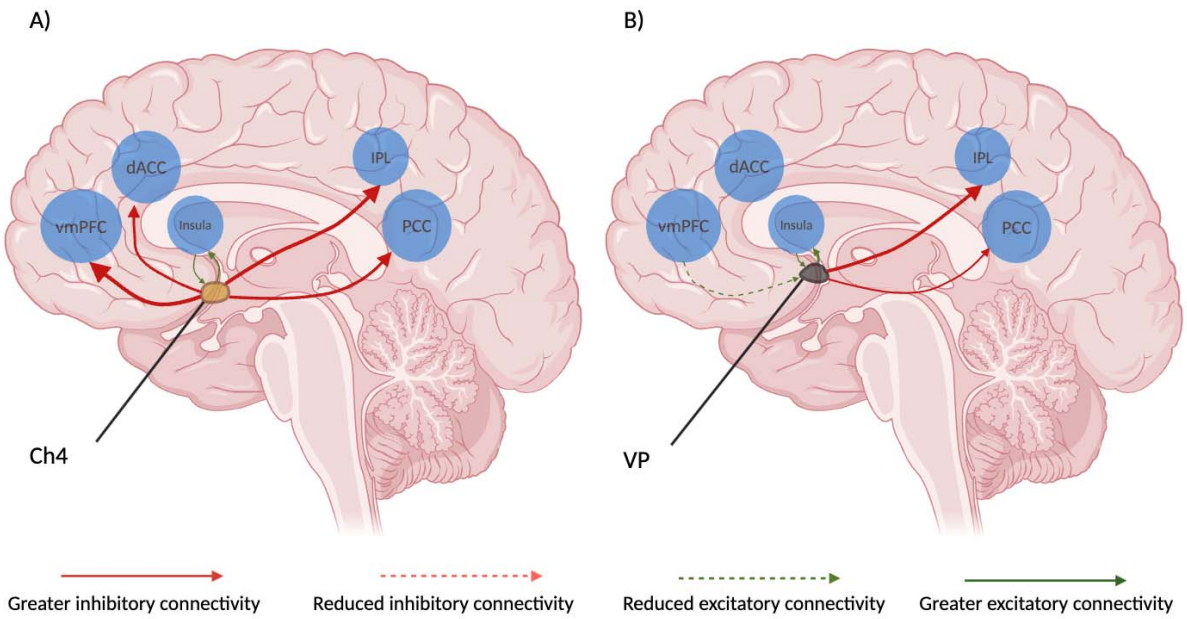

Figure 2. Differences in effective connectivity from the basal forebrain to cortical brain regions in clinical participants compared with healthy controls. Results indicate effects involving A) Ch4 (yellow) and B) ventral pallidum (black). Arrows have been weighted to indicate the relative size of the effects. Image created with BioRender (www.biorender.com).

Clinical participants additionally illustrated several notable effects involving Ch1-3, specifically reduced excitatory connectivity to the right IPL (-0.16 Hz) as well as reduced inhibitory connectivity to the right IPL (0.06 Hz). The vmPFC demonstrated greater self-inhibition (.13), whereas the PCC was observed to have reduced self-inhibition (-.16). See Supplementary Table S1 for a full list of connectivity parameters.

Leave-one-out Cross Validation

Given that connectivity alterations largely implicated Ch4 and VP, we then tested whether the size of the effect of group on the connectivity between these regions and cortical regions was sufficiently large to predict symptom severity. This analysis revealed that connectivity alterations involving cortical midline regions were associated with overall negative emotional

state (vmPFC/dACC: $r = 0.25$, $p < 0.05$; PCC: 0.15, $p < 0.05$), whereas connectivity involving lateralized regions such as the anterior insula ($r = -0.27$: $p = 0.99$) and IPL ($r = -0.02$, $p = 0.58$) were not. Using the altered connectivity of the vmPFC, dACC, PCC and basal forebrain regions together resulted in an overall correlation of $r = 0.31$, $p < 0.05$ (Figure 3). This overall effect did not appear to be driven any of the DASS subscales, with depressive ($r = 0.30$, $p < .05$), stress-tension ($r = 0.27$, $p < .05$), or anxiety symptoms ($r = 0.26$, $p < 0.05$) demonstrating similar correlations.

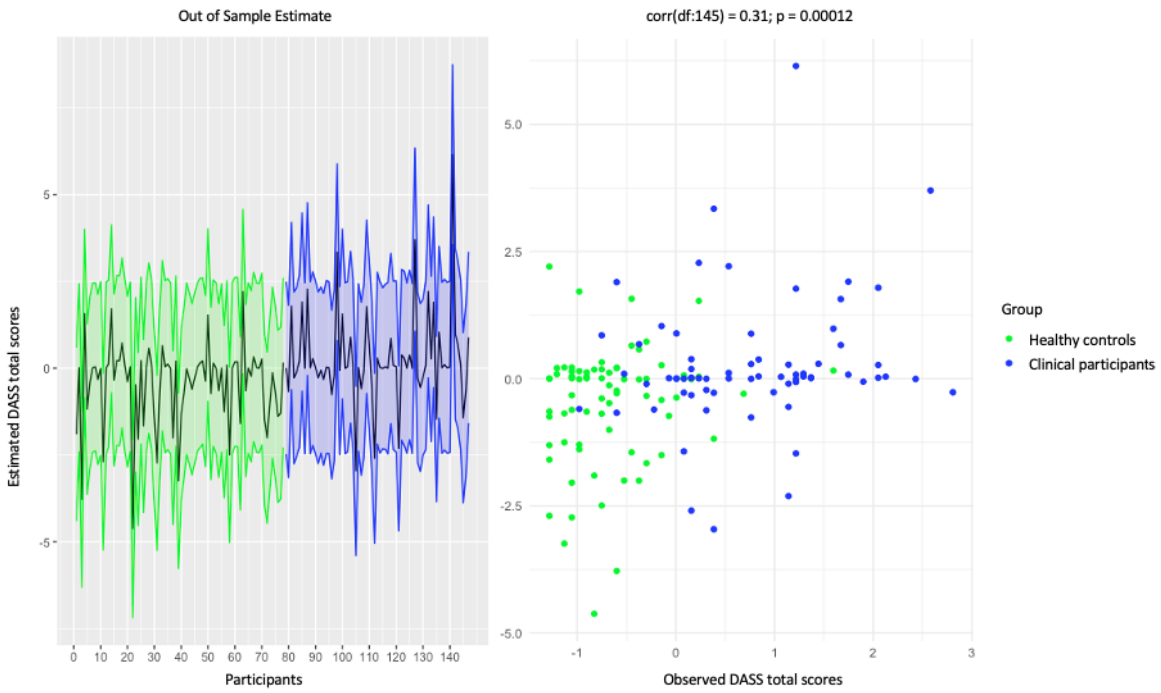

Figure 3. Leave-one-out cross-validation predicting DASS total scores for each participant. **Left:** The out-of-samples estimated of the DASS total score (z-scored) with 90% credible interval (shaded area). **Right:** The correlation between observed scores and the expected values for each individual participant using altered connections. Healthy controls are shown in green, clinical participants are shown in blue.

Discussion

This study examined alterations in basal forebrain resting-state effective connectivity in participants with depressive and anxiety disorders. Our findings highlight the differential roles of Ch1-3, Ch4, and VP in coordinating intrinsic brain networks. We identified that people with depressive and anxiety disorders demonstrated altered regulation of the DMN and salience networks stemming from Ch4 and VP. Notably, altered connections between the basal forebrain and cortical midline regions were predictive of participants' negative mood state. Our results both support the basal forebrain's role in the coordination of the DMN and salience network and demonstrate that alterations in this circuitry relate to broad negative affective symptoms.

The basal forebrain contains a heterogeneous population of neurons, including GABAergic, cholinergic, glutamatergic, and peptidergic neurons (Zaborszky et al. 1986; Walker et al. 1989; Zaborszky et al. 1999), which interact locally in addition to projecting cortically (Zaborszky and Duque 2000). Parvalbumin positive GABAergic neurons have emerged as likely candidates for the anatomical substrate of the basal forebrain responsible for DMN regulation (Kim et al. 2015; Zou et al. 2024). These GABAergic neurons have been shown to project to major DMN nodes, including the anterior cingulate and retrosplenial cortices (Do et al. 2016; Lozano-Montes et al. 2020). Optogenetic work has specifically identified causal evidence for the critical role of parvalbumin positive neurons in triggering state switching by activating the DMN and inducing associated behaviors (Lozano-Montes *et al*. 2020). These effects are also consistent with observations from VP GABAergic neurons, with stimulation of these neurons being shown to automatize internally focused behavior and impair attention directed towards external stimuli (Klaassen *et al*. 2021). This function mirrors increased ruminative thought observed across depressive and anxiety disorders (McLaughlin and Nolen-Hoeksema 2011). Moreover, local optogenetic inhibition of VP

GABAergic neurons triggers transitions from quiet wakefulness to exploratory behavior, with associated cortical activation being partially dependent on cholinergic transmission (Espinosa et al. 2019). Acetylcholine release and activity from cholinergic neurons in the basal forebrain have also been shown to be associated with reductions in DMN activity and connectivity (Peeters *et al.* 2020; Sanda et al. 2024). Together this indicates that regulation of the DMN likely occurs through both cholinergic and non-cholinergic mechanisms within the basal forebrain, consistent with findings from our current study.

Previous research has reported greater negative connectivity from the anterior DMN to regions of the salience and central executive networks in MDD (Jamieson *et al.* 2022), indicating an increased influence of the DMN on these other networks (Liu et al. 2023). These effects are congruent with research identifying that MDD is characterized by greater time spent in a coactivation pattern involving both activation of the DMN and deactivation of the frontoparietal network (Dong et al. 2024). This DMN dominance has been hypothesized to underlie a dysfunctional ability to shift attention from self-directed thoughts to external, goal-related behavior in MDD (Berman et al. 2011; Wang et al. 2016). Notably, the results of the current study and others indicate that these effects are directly influenced by changes in basal forebrain activity (Alves *et al.* 2019; Klaassen *et al.* 2021; Aguilar and McNally 2022). The fact that the largest effects were observed in regards to Ch4 connectivity is notable given its high proportion of cholinergic cells (Mesulam *et al.* 1983). The cholinergic basal forebrain system has been hypothesized to modulate information processing and attention by enhancing functional segregation within the brain (Shine 2019). This is further corroborated by more recent research which has shown that local inactivation of Ch4 leads to a decrease in the energy barriers required for a state transition in cortical activity, thereby increasing the likelihood of transitioning between different brain states (Munn et al. 2021; Taylor et al. 2024). Dysfunction of the cholinergic system has been implicated in the development of

cognitive impairments consistent with depression and anxiety symptoms, including attentional deficits, memory dysfunction, and negativity biases (Dagyte et al. 2011; Shackman et al. 2016). This association with negativity bias may, in part, explain the relationship between Ch4 circuitry dysfunction and broad negative mood symptoms highlighted above. As such, a combination of abnormal influences from both the VP and Ch4 may result in altered DMN activity and an impaired ability to switch between network states (Aguilar and McNally 2022), which in turn contributes to the development of depression and anxiety symptoms.

Dysfunctional Ch4 connectivity across these disorders may have direct implications for treatment using medications that affect cholinergic transmission. Scopolamine is a nonspecific muscarinic receptor antagonist which has demonstrated some evidence as a rapid antidepressant, with effects occurring as quickly as 3 days post-infusion (Furey and Drevets 2006; Jaffe et al. 2013). However, there have been relatively few high-quality trials investigating scopolamine's antidepressant effects and these studies have demonstrated inconsistent evidence for its effectiveness due to differences in administration routes and dosage (Furey and Drevets 2006; Mocko et al. 2023). This observed variability in response may also be indicative of a specific underlying biotype which demonstrates sensitivity to this treatment. Relatively few investigations have been undertaken to identify potential predictors of improved treatment response to scopolamine (Drevets et al. 2020). However, growing evidence indicates that scopolamine's rapid antidepressant effects, akin to other rapid antidepressant such as ketamine, occurs via inhibition of GABAergic interneurons in the mPFC (Fogaça et al. 2021). Given the highlighted role of the basal forebrain in coordinating the activity of the DMN and changes in this circuitry in depressive and anxiety disorders, investigation into the utility of these connectivity alterations in predicting response to scopolamine is warranted.

Limitations

While the transdiagnostic nature of the clinical group under investigation is a strength of the study and is representative of community samples, using discrete diagnostic categories to investigate this circuitry and its relationship with specific symptoms may be more useful in identifying specific clinical targets. Notably, 15 participants were excluded from our analysis due in insufficient mapping of BOLD signal in one or more of the regions, which was largely driven by signal dropout in basal forebrain subregions and potentially introduces a risk of selection bias. While 7T fMRI has many advantages over 3T, it also has several notable drawbacks including increased susceptibility artifacts which may have contributed to this issue (Beisteiner et al. 2011). Given the role of the cholinergic system in modulating arousal and attention (Larsen and Waters 2018), physiological measure such as eye tracking may have provided greater insight into the discrete time periods in which this circuitry was most active and as such should be integrated into future research. Additionally, assessment of negative symptoms was limited to the DASS. While this is a well validated measure (Page et al. 2007), it offers less specificity than other assessments of depressive and anxiety symptoms. Assessments of other transdiagnostic features related to basal forebrain functioning such as negativity bias, attentional impairments, and sleep dysfunction may provide greater insights into dysfunction implicated by these results.

Conclusions

To our knowledge, this is the first study to examine alterations in basal forebrain subregion effective connectivity in people with depressive and anxiety disorders. This work supports the notion that the basal forebrain is an important functional regulator of intrinsic brain networks and that different subregions have unique relationships with these networks. We identified

widespread increased inhibition from Ch4 to regions of the DMN and the dACC. Similar alterations were observed from the VP to regions of the posterior DMN. Dysfunction between these basal forebrain subregions and cortical midline regions were observed to be predictive of non-specific negative mood states. While a putative cholinergic basis of the aforementioned dysfunction needs to be established through future research, this may have implications for novel treatment targeting in depressive and anxiety disorders.

Declaration of Competing and Financial Interests

The authors declare no biomedical financial interests or potential conflicts of interest.

Funding

This study was supported by National Health and Medical Research Council of Australia (NHMRC) Project Grants (1161897) to BJH and (1073041) to KLF. TS is supported by a NHMRC/MRFF Investigator Grant (MRF1193736), a BBRF Young Investigator Grant, and a University of Melbourne McKenzie Fellowship. JA and SI are supported by Australian Government Research Training Program Scholarships.

Acknowledgements

The authors thank Braden Thai, Holly Carey and Amy Nielson for their contributions to data collection. The authors also acknowledge the facilities and scientific and technical assistance of the National Imaging Facility, a National Collaborative Research Infrastructure Strategy (NCRIS) capability, at the Melbourne Brain Centre Imaging Unit, University of Melbourne. In addition, the authors are grateful to Siemens for providing the MP2RAGE sequence as a “works in progress package” and CMRR (University of Minnesota) for sharing the multiband EPI sequence.

References

Aguilar DD, McNally JM. 2022. Subcortical control of the default mode network: Role of the basal forebrain and implications for neuropsychiatric disorders. Brain Res Bull. 185:129-139.

Alves PN, Foulon C, Karolis V, Bzdok D, Margulies DS, Volle E, Thiebaut de Schotten M. 2019. An improved neuroanatomical model of the default-mode network reconciles previous neuroimaging and neuropathological findings. Commun Biol. 2:370.

Ashburner J. 2007. A fast diffeomorphic image registration algorithm. Neuroimage. 38:95-113.

Behzadi Y, Restom K, Liau J, Liu TT. 2007. A component based noise correction method (CompCor) for BOLD and perfusion based fMRI. Neuroimage. 37:90-101.

Beisteiner R, Robinson S, Wurnig M, Hilbert M, Merksa K, Rath J, Höllinger I, Klinger N, Marosi C, Trattnig S, Geissler A. 2011. Clinical fMRI: evidence for a 7T benefit over 3T. Neuroimage. 57:1015-1021.

Berman MG, Nee DE, Casement M, Kim HS, Deldin P, Kross E, Gonzalez R, Demiralp E, Gotlib IH, Hamilton P, Joormann J, Waugh C, Jonides J. 2011. Neural and behavioral effects of interference resolution in depression and rumination. Cogn Affect Behav Ne. 11:85-96.

Bertocci MA, Afriyie-Agyemang Y, Rozovsky R, Iyengar S, Stiffler R, Aslam HA, Bebko G, Phillips ML. 2023. Altered patterns of central executive, default mode and salience network activity and connectivity are associated with current and future depression risk in two independent young adult samples. Mol Psychiatry. 28:1046-1056.

Birn RM, Smith MA, Jones TB, Bandettini PA. 2008. The respiration response function: the temporal dynamics of fMRI signal fluctuations related to changes in respiration. Neuroimage. 40:644-654.

Cabrera SM, Chavez CM, Corley SR, Kitto MR, Butt AE. 2006. Selective lesions of the nucleus basalis magnocellularis impair cognitive flexibility. Behav Neurosci. 120:298-306.

Chang C, Cunningham JP, Glover GH. 2009. Influence of heart rate on the BOLD signal: the cardiac response function. Neuroimage. 44:857-869.

Chen L, Ke Y, Ma H, Gao L, Zhou Y, Zhu H, Liu H, Zhang F, Zhou W. 2021. Fluoxetine and Ketamine Reverse the Depressive but Not Anxiety Behavior Induced by Lesion of Cholinergic Neurons in the Horizontal Limb of the Diagonal Band of Broca in Male Rat. Front Behav Neurosci. 15:602708.

Dagyte G, Den Boer JA, Trentani A. 2011. The cholinergic system and depression. Behav Brain Res. 221:574-582.

Do JP, Xu M, Lee SH, Chang WC, Zhang S, Chung S, Yung TJ, Fan JL, Miyamichi K, Luo L, Dan Y. 2016. Cell type-specific long-range connections of basal forebrain circuit. Elife. 5.

Dong D, Pizzagalli DA, Bolton TAW, Ironside M, Zhang X, Li C, Sun X, Xiong G, Cheng C, Wang X, Yao S, Belleau EL. 2024. Sex-specific resting state brain network dynamics in patients with major depressive disorder. Neuropsychopharmacology. 49:806-813.

Dosenbach NU, Fair DA, Miezin FM, Cohen AL, Wenger KK, Dosenbach RA, Fox MD, Snyder AZ, Vincent JL, Raichle ME, Schlaggar BL, Petersen SE. 2007. Distinct brain networks for adaptive and stable task control in humans. Proc Natl Acad Sci U S A. 104:11073-11078.

Drevets WC, Bhattacharya A, Furey ML. 2020. Chapter Twelve - The antidepressant efficacy of the muscarinic antagonist scopolamine: Past findings and future directions. In: Duman RS, Krystal JH, editors. Advances in Pharmacology Academic Press p 357-386.

Dulawa SC, Janowsky DS. 2019. Cholinergic regulation of mood: from basic and clinical studies to emerging therapeutics. Mol Psychiatry. 24:694-709.

Dutta A, McKie S, Deakin JF. 2014. Resting state networks in major depressive disorder. Psychiatry Res. 224:139-151.

Edlow BL, Mareyam A, Horn A, Polimeni JR, Witzel T, Tisdall MD, Augustinack JC, Stockmann JP, Diamond BR, Stevens A. 2019. 7 Tesla MRI of the ex vivo human brain at 100 micron resolution. Scientific data. 6:244.

Espinosa N, Alonso A, Morales C, Espinosa P, Chavez AE, Fuentealba P. 2019. Basal Forebrain Gating by Somatostatin Neurons Drives Prefrontal Cortical Activity. Cereb Cortex. 29:42-53.

Fair DA, Cohen AL, Power JD, Dosenbach NUF, Church JA, Miezin FM, Schlaggar BL, Petersen SE. 2009. Functional Brain Networks Develop from a "Local to Distributed" Organization. Plos Computational Biology. 5.

Fogaça MV, Wu M, Li C, Li XY, Picciotto MR, Duman RS. 2021. Inhibition of GABA interneurons in the mPFC is sufficient and necessary for rapid antidepressant responses. Mol Psychiatry. 26:3277-3291.

Friston KJ, Harrison L, Penny W. 2003. Dynamic causal modelling. Neuroimage. 19:1273-1302.

Friston KJ, Litvak V, Oswal A, Razi A, Stephan KE, van Wijk BCM, Ziegler G, Zeidman P. 2016. Bayesian model reduction and empirical Bayes for group (DCM) studies. Neuroimage. 128:413-431.

Friston KJ, Penny W. 2011. Post hoc Bayesian model selection. Neuroimage. 56:2089-2099.

Fritz HCJ, Ray N, Dyrba M, Sorg C, Teipel S, Grothe MJ. 2019. The corticotopic organization of the human basal forebrain as revealed by regionally selective functional connectivity profiles. Human Brain Mapping. 40:868-878.

Furey ML, Drevets WC. 2006. Antidepressant efficacy of the antimuscarinic drug scopolamine: a randomized, placebo-controlled clinical trial. Arch Gen Psychiatry. 63:1121-1129.

Glover GH, Li TQ, Ress D. 2000. Image-based method for retrospective correction of physiological motion effects in fMRI: RETROICOR. Magn Reson Med. 44:162-167.

Harrison BJ, Davey CG, Savage HS, Jamieson AJ, Leonards CA, Moffat BA, Glarin RK, Steward T. 2022. Dynamic subcortical modulators of human default mode network function. Cereb Cortex. 32:4345-4355.

Herman AM, Ortiz-Guzman J, Kochukov M, Herman I, Quast KB, Patel JM, Tepe B, Carlson JC, Ung K, Selever J, Tong Q, Arenkiel BR. 2016. A cholinergic basal forebrain feeding circuit modulates appetite suppression. Nature. 538:253-256.

Jaffe RJ, Novakovic V, Peselow ED. 2013. Scopolamine as an Antidepressant: A Systematic Review. Clin Neuropharmacol. 36:24-26.

Jamieson AJ, Harrison BJ, Delahoy R, Schmaal L, Felmingham KL, Phillips L, Davey CG. 2023. A brain model of altered self-appraisal in social anxiety disorder. Transl Psychiatry. 13:344.

Jamieson AJ, Harrison BJ, Razi A, Davey CG. 2022. Rostral anterior cingulate network effective connectivity in depressed adolescents and associations with treatment response in a randomized controlled trial. Neuropsychopharmacology. 47:1240-1248.

Kasper L, Bollmann S, Diaconescu AO, Hutton C, Heinzle J, Iglesias S, Hauser TU, Sebold M, Manjaly ZM, Pruessmann KP, Stephan KE. 2017. The PhysIO Toolbox for Modeling Physiological Noise in fMRI Data. J Neurosci Meth. 276:56-72.

Keuken MC, Isaacs BR, Trampel R, van der Zwaag W, Forstmann BU. 2018. Visualizing the Human Subcortex Using Ultra-high Field Magnetic Resonance Imaging. Brain Topogr. 31:513-545.

Kim T, Thankachan S, McKenna JT, McNally JM, Yang C, Choi JH, Chen L, Kocsis B, Deisseroth K, Strecker RE, Basheer R, Brown RE, McCarley RW. 2015. Cortically projecting basal forebrain parvalbumin neurons regulate cortical gamma band oscillations. Proc Natl Acad Sci U S A. 112:3535-3540.

Klaassen A-L, Heiniger A, Sánchez PV, Harvey MA, Rainer G. 2021. Ventral pallidum regulates the default mode network, controlling transitions between internally and externally guided behavior. Proceedings of the National Academy of Sciences of the United States of America. 118:1-10.

Knowland D, Lilascharoen V, Pacia CP, Shin S, Wang EH, Lim BK. 2017. Distinct Ventral Pallidal Neural Populations Mediate Separate Symptoms of Depression. Cell. 170:284-297 e218.

Lafayette L, Sauter G, Vu L, Meade B editors. Spartan Performance and Flexibility: An HPC-Cloud Chimera, OpenStack Summit; 2016 October 27, 2016; Barcelona.

Larsen RS, Waters J. 2018. Neuromodulatory Correlates of Pupil Dilation. Front Neural Circuits. 12:21.

Li CS, Ide JS, Zhang S, Hu S, Chao HH, Zaborszky L. 2014. Resting state functional connectivity of the basal nucleus of Meynert in humans: in comparison to the ventral striatum and the effects of age. Neuroimage. 97:321-332.

Li R, Shen F, Sun X, Zou T, Li L, Wang X, Deng C, Duan X, He Z, Yang M, Li Z, Chen H. 2023. Dissociable salience and default mode network modulation in generalized anxiety disorder: a connectome-wide association study. Cereb Cortex. 33:6354-6365.

Liu C, Belleau EL, Dong D, Sun X, Xiong G, Pizzagalli DA, Auerbach RP, Wang X, Yao S. 2023. Trait- and state-like co-activation pattern dynamics in current and remitted major depressive disorder. J Affect Disord. 337:159-168.

Lovibond SH. 1995. Manual for the depression anxiety stress scales. Sydney psychology foundation.

Lozano-Montes L, Dimanico M, Mazloum R, Li W, Nair J, Kintscher M, Schneggenburger R, Harvey M, Rainer G. 2020. Optogenetic Stimulation of Basal Forebrain Parvalbumin Neurons Activates the Default Mode Network and Associated Behaviors. Cell Rep. 33:108359.

Marques JP, Kober T, Krueger G, van der Zwaag W, Van de Moortele PF, Gruetter R. 2010. MP2RAGE, a self bias-field corrected sequence for improved segmentation and T1-mapping at high field. Neuroimage. 49:1271-1281.

McLaughlin KA, Nolen-Hoeksema S. 2011. Rumination as a transdiagnostic factor in depression and anxiety. Behav Res Ther. 49:186-193.

Mesulam MM, Mufson EJ, Levey AI, Wainer BH. 1983. Cholinergic innervation of cortex by the basal forebrain: cytochemistry and cortical connections of the septal area, diagonal band nuclei, nucleus basalis (substantia innominata), and hypothalamus in the rhesus monkey. J Comp Neurol. 214:170-197.

Mineur YS, Obayemi A, Wigestrand MB, Fote GM, Calarco CA, Li AM, Picciotto MR. 2013. Cholinergic signaling in the hippocampus regulates social stress resilience and anxiety- and depression-like behavior. Proceedings of the National Academy of Sciences of the United States of America. 110:3573-3578.

Mocko P, Sladowska K, Kawalec P, Babii Y, Pilc A. 2023. The Potential of Scopolamine as an Antidepressant in Major Depressive Disorder: A Systematic Review of Randomized Controlled Trials. Biomedicines. 11.

Moeller S, Yacoub E, Olman CA, Auerbach E, Strupp J, Harel N, Ugurbil K. 2010. Multiband multislice GE-EPI at 7 tesla, with 16-fold acceleration using partial parallel imaging with application to high spatial and temporal whole-brain fMRI. Magn Reson Med. 63:1144-1153.

Mohan A, Roberto AJ, Mohan A, Lorenzo A, Jones K, Carney MJ, Liogier-Weyback L, Hwang S, Lapidus KA. 2016. The Significance of the Default Mode Network (DMN) in Neurological and Neuropsychiatric Disorders: A Review. Yale J Biol Med. 89:49-57.

Mulders PC, van Eijndhoven PF, Schene AH, Beckmann CF, Tendolkar I. 2015. Resting-state functional connectivity in major depressive disorder: A review. Neurosci Biobehav Rev. 56:330-344.
Munn BR, Muller EJ, Wainstein G, Shine JM. 2021. The ascending arousal system shapes neural dynamics to mediate awareness of cognitive states. Nat Commun. 12:6016.
Nair J, Klaassen AL, Arato J, Vyssotski AL, Harvey M, Rainer G. 2018. Basal forebrain contributes to default mode network regulation. Proc Natl Acad Sci U S A. 115:1352-1357.
Novelli L, Friston K, Razi A. 2024. Spectral dynamic causal modeling: A didactic introduction and its relationship with functional connectivity. Netw Neurosci. 8:178-202.
O'Brien KR, Kober T, Hagmann P, Maeder P, Marques J, Lazeyras F, Krueger G, Roche A. 2014. Robust T1-weighted structural brain imaging and morphometry at 7T using MP2RAGE. PLoS One. 9:e99676.
Page AC, Hooke GR, Morrison DL. 2007. Psychometric properties of the Depression Anxiety Stress Scales (DASS) in depressed clinical samples. Br J Clin Psychol. 46:283-297.
Pauli WM, Nili AN, Tyszka JM. 2018. A high-resolution probabilistic in vivo atlas of human subcortical brain nuclei. Sci Data. 5:180063.
Peeters LM, van den Berg M, Hinz R, Majumdar G, Pintelon I, Keliris GA. 2020. Cholinergic Modulation of the Default Mode Like Network in Rats. iScience. 23:101455.
Rabany L, Diefenbach GJ, Bragdon LB, Pittman BP, Zertuche L, Tolin DF, Goethe JW, Assaf M. 2017. Resting-State Functional Connectivity in Generalized Anxiety Disorder and Social Anxiety Disorder: Evidence for a Dimensional Approach. Brain Connect. 7:289-298.
Root DH, Melendez RI, Zaborszky L, Napier TC. 2015. The ventral pallidum: Subregion-specific functional anatomy and roles in motivated behaviors. Prog Neurobiol. 130:29-70.
Rosa MJ, Friston KJ, Penny W. 2012. Post-hoc selection of dynamic causal models. J Neurosci Meth. 208:66-78.
Sanda P, Hlinka J, van den Berg M, Skoch A, Bazhenov M, Keliris GA, Krishnan GP. 2024. Cholinergic modulation supports dynamic switching of resting state networks through selective DMN suppression. PLoS Comput Biol. 20:e1012099.
Shackman AJ, Stockbridge MD, Tillman RM, Kaplan CM, Tromp DP, Fox AS, Gamer M. 2016. The neurobiology of dispositional negativity and attentional biases to threat: Implications for understanding anxiety disorders in adults and youth. J Exp Psychopathol. 7:311-342.
Sheehan DV, Lecrubier Y, Sheehan KH, Amorim P, Janavs J, Weiller E, Hergueta T, Baker R, Dunbar GC. 1998. The Mini-International Neuropsychiatric Interview (MINI): the development and validation of a structured diagnostic psychiatric interview for DSM-IV and ICD-10. J Clin Psychiat. 59:22-33.
Shine JM. 2019. Neuromodulatory Influences on Integration and Segregation in the Brain. Trends Cogn Sci. 23:572-583.
Sridharan D, Levitin DJ, Menon V. 2008. A critical role for the right fronto-insular cortex in switching between central-executive and default-mode networks. Proceedings of the National Academy of Sciences of the United States of America. 105:12569-12574.
Taylor NL, Whyte CJ, Munn BR, Chang C, Lizier JT, Leopold DA, Turchi JN, Zaborszky L, Muller EJ, Shine JM. 2024. Causal evidence for cholinergic stabilization of attractor landscape dynamics. Cell Rep. 43:114359.
Tolin D, Bowe W, Davis E, Hannan S, Springer K, Worden B, Steinman S. 2016. Diagnostic Interview for anxiety, mood, and OCD and related neuropsychiatric disorders (DIAMOND). Hartford, CT: The Institute of Living, Hartford Healthcare Corporation.
Walker LC, Koliatsos VE, Kitt CA, Richardson RT, Rokaeus A, Price DL. 1989. Peptidergic neurons in the basal forebrain magnocellular complex of the rhesus monkey. J Comp Neurol. 280:272-282.

Wang X, Ongur D, Auerbach RP, Yao SQ. 2016. Cognitive Vulnerability to Major Depression: View from the Intrinsic Network and Cross-network Interactions. Harvard Rev Psychiat. 24:188-201.

Wilke M. 2012. An alternative approach towards assessing and accounting for individual motion in fMRI timeseries. Neuroimage. 59:2062-2072.

Xu L, Xu H, Ding H, Li J, Wang C. 2021. Intrinsic Network Brain Dysfunction Correlates With Temporal Complexity in Generalized Anxiety Disorder and Panic Disorder. Front Hum Neurosci. 15:647518.

Yamakawa GR, Basu P, Cortese F, MacDonnell J, Whalley D, Smith VM, Antle MC. 2016. The cholinergic forebrain arousal system acts directly on the circadian pacemaker. Proc Natl Acad Sci U S A. 113:13498-13503.

Yarkoni T, Poldrack RA, Nichols TE, Van Essen DC, Wager TD. 2011. Large-scale automated synthesis of human functional neuroimaging data. Nat Methods. 8:665-670.

Yuan R, Biswal BB, Zaborszky L. 2019. Functional Subdivisions of Magnocellular Cell Groups in Human Basal Forebrain: Test-Retest Resting-State Study at Ultra-high Field, and Meta-analysis. Cereb Cortex. 29:2844-2858.

Zaborszky L, Carlsen J, Brashear HR, Heimer L. 1986. Cholinergic and GABAergic afferents to the olfactory bulb in the rat with special emphasis on the projection neurons in the nucleus of the horizontal limb of the diagonal band. J Comp Neurol. 243:488-509.

Zaborszky L, Duque A. 2000. Local synaptic connections of basal forebrain neurons. Behavioural Brain Research. 115:143-158.

Zaborszky L, Hoemke L, Mohlberg H, Schleicher A, Amunts K, Zilles K. 2008. Stereotaxic probabilistic maps of the magnocellular cell groups in human basal forebrain. Neuroimage. 42:1127-1141.

Zaborszky L, Pang K, Somogyi J, Nadasdy Z, Kallo I. 1999. The basal forebrain corticopetal system revisited. Ann N Y Acad Sci. 877:339-367.

Zeidman P, Jafarian A, Seghier ML, Litvak V, Cagnan H, Price CJ, Friston KJ. 2019. A guide to group effective connectivity analysis, part 2: Second level analysis with PEB. Neuroimage. 200:12-25.

Zhang X, Yang X, Wu B, Pan N, He M, Wang S, Kemp GJ, Gong Q. 2023. Large-scale brain functional network abnormalities in social anxiety disorder. Psychol Med. 53:6194-6204.

Zhao Y, Kirschenhofer T, Harvey M, Rainer G. 2024. Mediodorsal thalamus and ventral pallidum contribute to subcortical regulation of the default mode network. Commun Biol. 7:891.

Zou Y, Tong C, Peng W, Qiu Y, Li J, Xia Y, Pei M, Zhang K, Li W, Xu M, Liang Z. 2024. Cell-type-specific optogenetic fMRI on basal forebrain reveals functional network basis of behavioral preference. Neuron.